

Control of Polar Structure by Intermetallic Charge Transfer in Perovskite-Type Oxides

The polarity of crystal structures is successfully controlled by an intermetallic charge transfer between the constituent cations in perovskite-type $(1-x)\text{PbVO}_3\text{-}x\text{BiCoO}_3$ solid solutions. The end members of PbVO_3 and BiCoO_3 possess a PbTiO_3 -type tetragonal perovskite structure, while a nonpolar cubic perovskite-type structure is observed in $(1-x)\text{PbVO}_3\text{-}x\text{BiCoO}_3$ solid solutions ($0.40 \leq x \leq 0.75$). X-ray absorption spectroscopy (XAS) and magnetic measurements reveal that the change in crystal structure results from an intermetallic charge transfer, $\text{Co}^{3+} + \text{V}^{4+} \rightarrow \text{Co}^{2+} + \text{V}^{5+}$. This finding shows that tuning an electronic structure by making a solid solution is an effective way to control crystal structures, properties and functions.

The valence states of constituent cations in oxides characterize the nature of crystal structures and electronic properties. Interestingly, the valence states of cations in solid solutions and double-perovskite compounds occasionally differ from those in their parent compounds, which are determined by the difference in energy of valence levels. For example, double-perovskite-type $\text{Bi}_2\text{NiMnO}_6$ has the valence states of Bi^{3+} , Ni^{2+} , and Mn^{4+} , whereas the end members possess the states of $\text{Bi}^{3+}_{0.5}\text{Bi}^{5+}_{0.5}\text{Ni}^{2+}\text{O}_3$ (at ambient pressure) and $\text{Bi}^{3+}\text{Mn}^{3+}\text{O}_3$ [1-3].

PbVO_3 and BiCoO_3 possess polar perovskite-type structures with giant tetragonal distortion, which are isostructural with PbTiO_3 [4, 5]. They are synthesized under high-pressure and high-temperature conditions.

Their giant tetragonal distortions are generated as a result of the combination of *A*-site and *B*-site cations. The stereochemical activity of Pb^{2+} and Bi^{3+} and strong covalency of Pb-O and Bi-O stabilize the structural distortion, as in PbTiO_3 . The Jahn-Teller effect of V^{4+} ($3d^1$) and Co^{3+} ($3d^6$, high-spin) further enhances the tetragonality. As the result, the *c/a* ratio and spontaneous polarization reach respectively 1.23 and $101 \mu\text{C}/\text{cm}^2$ for PbVO_3 and 1.27 and $126 \mu\text{C}/\text{cm}^2$ for BiCoO_3 . Such large polarizations result in new functionalities, for example, electron-doped PbVO_3 , $\text{Pb}_{1-x}\text{Bi}_x\text{VO}_3$, is known as one of the highest negative thermal expansion materials [6]. A polar-to-nonpolar structural phase transition is observed in electron-doped PbVO_3 , which is accompanied by an insulator-to-metal transition and colossal volume shrink-

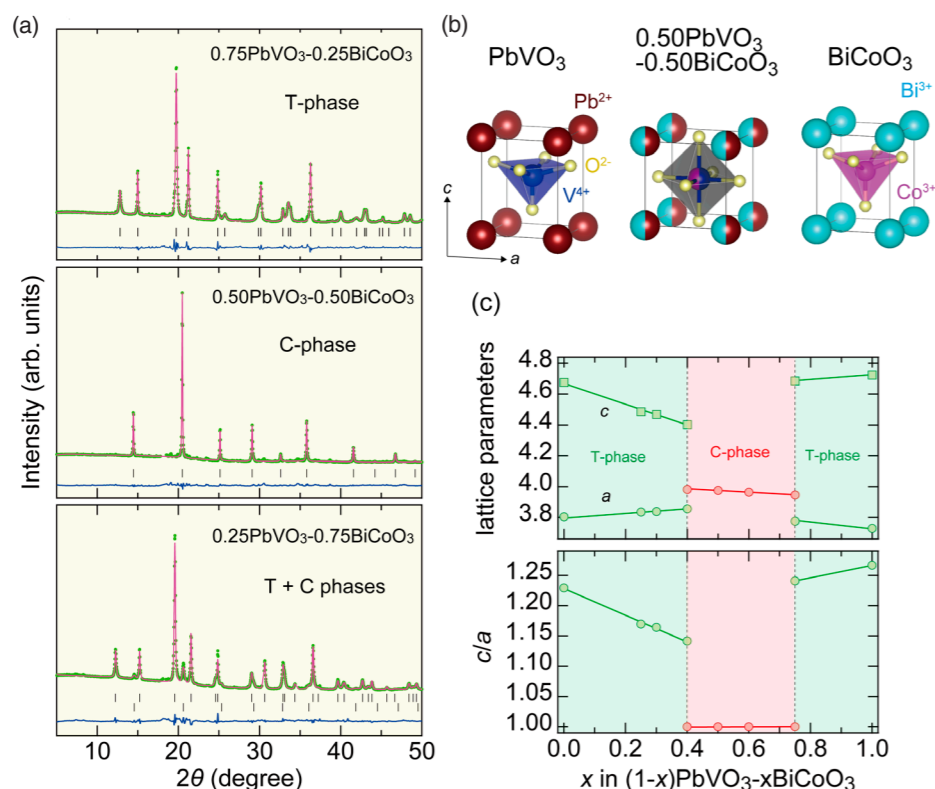


Figure 1: (a) Synchrotron X-ray diffraction patterns and results of Rietveld analysis for $0.75\text{PbVO}_3\text{-}0.25\text{BiCoO}_3$, $0.50\text{PbVO}_3\text{-}0.50\text{BiCoO}_3$, and $0.25\text{PbVO}_3\text{-}0.75\text{BiCoO}_3$ composites. Observed (red points) and calculated (blue line) SXRD patterns, and their difference (green line). The tick marks correspond to the position of Bragg reflections of the tetragonal $P4mm$ phase (top) and the cubic $Pm\text{-}3m$ phase (bottom). T and C stand for tetragonal and cubic phase, respectively. (b) Crystal structures of tetragonal phase (PbVO_3 and BiCoO_3) and cubic phase ($0.50\text{PbVO}_3\text{-}0.50\text{BiCoO}_3$). (c) Lattice parameters *a* and *c*, and *c/a* ratios of $(1-x)\text{PbVO}_3\text{-}x\text{BiCoO}_3$ solid solutions ($x = 0, 0.25, 0.30, 0.40, 0.50, 0.60, 0.75, \text{ and } 1.0$).

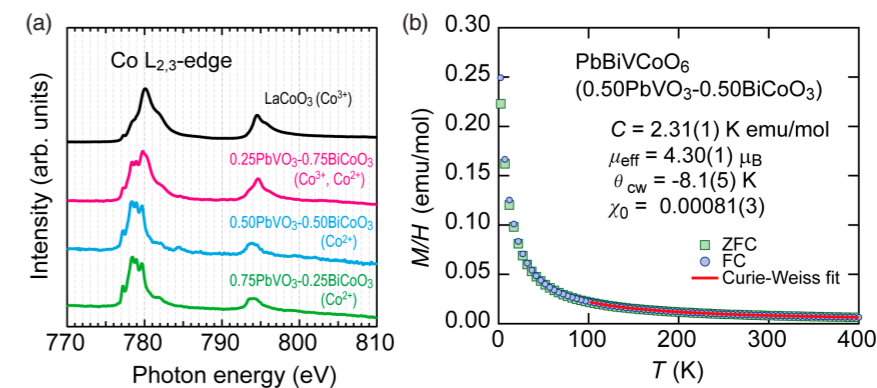


Figure 2: (a) XAS spectra of the Co $L_{2,3}$ -edge for LaCoO_3 (black, reference), $0.25\text{PbVO}_3\text{-}0.75\text{BiCoO}_3$ (pink), $0.50\text{PbVO}_3\text{-}0.50\text{BiCoO}_3$ (light blue), and $0.75\text{PbVO}_3\text{-}0.25\text{BiCoO}_3$ (green). (b) Temperature dependence of magnetization susceptibility of the $0.50\text{PbVO}_3\text{-}0.50\text{BiCoO}_3$ sample in a magnetic field of 0.1 T. The red curve between 100 K and 400 K features the results of fitting to the Curie-Weiss law.

age, -7.9% for $\text{Pb}_{0.8}\text{Bi}_{0.2}\text{VO}_3$ at 550–750 K. Thus far, we have revealed that the valence states of *B*-site cations significantly affected the stability of the polar structure in tetragonal perovskites [7, 8].

In this study, we clarified the evolution of crystal structures and electronic states of solid solutions between PbVO_3 and BiCoO_3 [$(1-x)\text{PbVO}_3\text{-}x\text{BiCoO}_3$]. The samples were successfully synthesized using a high-pressure and high-temperature method. Figure 1 (a) shows the synchrotron X-ray patterns and the results of Rietveld analysis. The data were collected at BL-8B. A nonpolar cubic perovskite structure (space group $Pm\text{-}3m$) was observed in the range of ($0.40 \leq x \leq 0.75$), whereas the tetragonal structure was preserved in the other ranges [Fig. 1 (b)]. The *c/a* ratio and spontaneous polarization systematically decreased toward the cubic region, as shown in Fig. 1 (c). Notably, the volume difference between tetragonal and cubic phases reached 3.7% for $0.60\text{PbVO}_3\text{-}0.40\text{BiCoO}_3$ and 8.7% for $0.25\text{PbVO}_3\text{-}0.75\text{BiCoO}_3$, paving the way for the realization of new negative thermal expansion materials.

In general, solid solutions between tetragonal perovskites with the same crystallographic symmetry ($P4mm$) preserve the original structure. The valence states of *B*-site cations were evaluated to reveal the mechanism of the change in crystal structure in $(1-x)\text{PbVO}_3\text{-}x\text{BiCoO}_3$ solid solutions. Figure 2 (a) shows the XAS spectra of the Co $L_{2,3}$ -edge for $0.25\text{PbVO}_3\text{-}0.75\text{BiCoO}_3$, $0.50\text{PbVO}_3\text{-}0.50\text{BiCoO}_3$, $0.75\text{PbVO}_3\text{-}0.25\text{BiCoO}_3$, and LaCoO_3 . Only Co^{2+} was observed in $0.50\text{PbVO}_3\text{-}0.50\text{BiCoO}_3$ and $0.75\text{PbVO}_3\text{-}0.25\text{BiCoO}_3$, whereas both Co^{2+} and Co^{3+} coexisted in $0.25\text{PbVO}_3\text{-}0.75\text{BiCoO}_3$. Figure 2 (b) depicts the temperature dependence of magnetization susceptibility of the $0.50\text{PbVO}_3\text{-}0.50\text{BiCoO}_3$ sample. The Curie-Weiss fitting between 100 K and 400 K gave the square of the effective magnetic moment of $\mu_{\text{eff}}^2 = 18.49(1) \mu_B^2$ and the Weiss temperature of $\theta_w = -8.1(5)$ K. The obtained value of μ_{eff}^2 is close to the theoretical value expected for the combination of Co^{2+} (high-spin state, $3d^7$) and V^{5+} ($3d^0$) with $g = 2$. The

low q_w value also corroborates the partial existence of nonmagnetic cation. The valence states are different from the end members, $\text{BiCo}^{3+}\text{O}_3$ and $\text{PbV}^{4+}\text{O}_3$.

To summarize the above results, an intermetallic charge transfer, $\text{Co}^{3+} + \text{V}^{4+} \rightarrow \text{Co}^{2+} + \text{V}^{5+}$, occurs in $(1-x)\text{PbVO}_3\text{-}x\text{BiCoO}_3$ solid solutions. Given that neither Co^{2+} nor V^{5+} are Jahn-Teller active, the intermetallic charge transfer triggers the polar-to-nonpolar change in crystal structure. The decrease in *c/a* ratio with increasing solid solution ratio from both sides is caused by the self-doping effect. The intermetallic charge transfer is ascribed to the difference in depth of 3d-level of each cation. In conclusion, we have found a new way to control the polar crystal structure by making the solid solution. This finding paves the way for the development of new functional materials.

REFERENCES

- [1] M. Azuma, K. Takata, T. Saito, S. Ishiwata, Y. Shimakawa and M. Takano, *J. Am. Chem. Soc.* **127**, 8889 (2005).
- [2] S. Ishiwata, M. Azuma, M. Takano, E. Nishibori, M. Takata, M. Sakata and K. Kato, *J. Mater. Chem.* **12**, 3733 (2002).
- [3] F. Sugawara, S. Iiida, Y. Syono and S. Akimoto, *J. Phys. Soc. Jpn.* **25**, 1553 (1968).
- [4] R. V. Shpanchenko, V. V. Chernaya, A. A. Tsirlin, P. S. Chizhov, D. E. Sklovsky, E. V. Antipov, E. P. Khlybov, V. Pomjakushin, A. M. Balagurov, J. E. Medvedeva, E. E. Kaul and C. Geibel, *Chem. Mater.* **16**, 3267 (2004).
- [5] A. A. Belik, S. Iikubo, K. Kodama, N. Igawa, S. Shamoto, S. Niitaka, M. Azuma, Y. Shimakawa, M. Takano, F. Izumi and E. Takayama-Muromachi, *Chem. Mater.* **18**, 798 (2006).
- [6] H. Yamamoto, T. Imai, Y. Sakai and M. Azuma, *Angew. Chem. Int. Ed.* **57**, 8170 (2018).
- [7] H. Yamamoto, T. Ogata, Y. Sakai and M. Azuma, *Inorg. Chem.* **58**, 2755 (2019).
- [8] H. Ishizaki, H. Yamamoto, T. Nishikubo, Y. Sakai, S. Kawaguchi, K. Yokoyama, Y. Okimoto, S. Koshihara, T. Yamamoto and M. Azuma, *Inorg. Chem.* **58**, 16059 (2019).

BEAMLINE

BL-8B

H. Yamamoto and H. Kimura (Tohoku Univ.-IMRAM)